ISSN 1392-1320 MATERIALS SCIENCE (MEDŽIAGOTYRA). Vol. XX, No. X. 2025

Microstructure and Visible Light Photocatalytic Studies of CeO_2 Doped ZnO Nanoparticles

Liangdong SUN [1], Zhifei YANG [1] *, Guojun SONG [1], Zheng GU [1, 2], Peiyao LI [1], Balakrishnan GOVINDASAMY [3]

[1] *College of Materials Science and Engineering, Qingdao University, Qingdao- 266071, China*
[2] *Weihai Innovation Institute, Qingdao University, Weihai- 264200, China*
[3] *Saveetha Institute of Medical and Technical Sciences, Saveetha Dental College and Hospital, Chennai-600077, Tamilnadu, India*

http://doi.org/10.5755/j02.ms.38408

Received 8 August 2024; accepted 5 September 2024

Cerium oxide (CeO_2) doped with zinc oxide (ZnO) nanoparticles were synthesised using sol-gel method. The impact of CeO_2 doping on the microstructure, optical, photocatalytic, and antibacterial properties of ZnO nanoparticles (NPs) were investigated. XRD results showed the presence of both CeO_2 and ZnO phases. The ZnO sample crystallizes into a hexagonal wurtzite structure and CeO_2 with a cubic structure. The crystallite sizes were estimated and found to be 18 nm and 29 nm for the CeO_2 and ZnO, nanoparticles respectively. FTIR spectrum reveals the formation of chemical bonds. The FESEM studies showed the formation of dense crystallites with aggregation. The EDX studies confirmed the presence of cerium, zinc, and oxygen in the sample, and no additional peaks have been detected. The UV-Visible spectroscopy analysis revealed the bandgap of 3.15 eV. The photodegradation activity of the nanoparticles with methylene blue (MB) dye was carried out using visible light irradiation and the degradation efficiency was found to be 75.81 % in 1 h duration. The antibacterial susceptibility test was conducted using the agar well diffusion method to investigate the activity of CeO_2 doped ZnO nanoparticles against E. coli, Salmonella typhimurium, Bacillus cereus, and Shigella flexneri, and the results showed significant antibacterial activity as compared to the control drug penicillin.
Keywords: cerium oxide, zinc oxide, XRD, antibacterial, photocatalytic activity, nanoparticles.

1. INTRODUCTION

The unique features and prospective applications of cerium oxide (CeO_2) doped zinc oxide (ZnO) nanoparticles make them highly interesting in numerous domains. Both CeO_2 and ZnO nanoparticles have undergone thorough examination and have been widely employed in several fields including catalysis, electronics, photonics, biomedical engineering, and environmental remediation. In recent decades, water contaminants originating from dyes and the textile industries emerged as a significant environmental concern. The discharge of surplus dyes into water sources has a detrimental impact on human life and the environment. Photocatalytic activity is a widely used technology that efficiently addresses this problem [1]. There are many metal oxide materials used for the photocatalytic degradation of different dyes [2, 3]. Among them, ZnO nanomaterial is an exceptional nanocatalyst, and the incorporation of rare earth (RE) metals can significantly enhance its catalytic activity. These factors pose significant challenges to enhance the photocatalytic efficiency of ZnO [4]. The photocatalytic activity depends on many parameters such as band-gap, number of charge carriers, and charge separation, and so on. Several researchers have conducted studies on metal doping using various procedures in order to enhance photocatalytic performance [5 – 8]. Recently, RE metals such as Er, Eu, and La have been utilised as dopants in ZnO [9, 10].

CeO_2 is a rare earth oxide, and has garnered significant interest due to its distinctive catalytic capabilities in redox processes. Additionally, the redox pair Ce^{3+}/Ce^{4+} of CeO_2 can switch back and forth quickly and reversibly. This characteristic gives it a high level of catalytic activity and electron transfer rate [11]. CeO_2 is a RE material with excellent catalytic properties and high oxygen storage capacity. When doped into ZnO nanoparticles, CeO_2 can modify their electronic and optical properties, making them suitable for various applications. Also, CeO_2 has been investigated for its photocatalytic properties, which can be beneficial for applications in water purification and air pollution control [12]. Additionally, CeO_2 doping can enhance the electrical conductivity of ZnO nanoparticles, making them promising for applications in transparent conductive films, solar cells, corrosion resistant coatings, and optoelectronic devices. Overall, the combination of CeO_2 and ZnO nanoparticles offers exciting possibilities for innovation and advancement in various fields [13].

There are only a few research articles on CeO_2 doped ZnO used for photocatalytic and antibacterial applications [14]. Shen et al. synthesised the cerium doped ZnO for the degradation of RhB dye. The experiment showed a degradation of 85.1 % in 125 min [15]. The researchers found that the introduction of RE doping in ZnO can create various imperfections, which can adjust the bandgap to a lower energy level. This adjustment allows visible light to be utilised as a source of illumination. In addition, the

* Corresponding author. Tel.: +86-18660260209.
E-mail: *zhifeiyang@qdu.edu.cn* (Z. Yang)

presence of RE ion dopants can enhance photocatalytic activity by effectively capturing and preventing electron recombination. Chatchai Rodwihok et al [1] prepared the CeO_2 doped ZnO nanoparticles by hydrothermal method and results showed that MO degradation activity increased with an increase of Ce doping under fluorescent lamp illumination. Syed et al prepared the nanocomposite and showed a degradation efficiency of 88 % when exposed to sunshine and 92 % to UV radiation [16].

CeO_2-ZnO NC demonstrated significant antibacterial action against a harmful bacterial strain [17]. Treating infections caused by intracellular bacteria and drug-resistant strains is challenging when employing antibiotics due to the limited ability of medications to cross cell membranes. Drugs that are of average size have minimal impact on microorganisms that are located inside cells. An alternative therapeutic approach has been suggested to address this constraint, involving the use of drug-loaded nanoparticles as intermediaries. Most forms of nanoparticles are of such small size that they can be readily phagocytosed by phagocytes in the host. Furthermore, the configurations of various kinds of nanoparticles (NPs) are well suited for transporting medications, and the adaptability of NPs to penetrate host cells through endocytosis enables a significant portion of the drug to be released within the cells. Therefore, it is of interest to study the antibacterial effect of CeO_2/ZnO NPs. The results indicate that the nanoparticles possess significant antimicrobial activity on certain selected bacteria [18].

Natural products have shown extensive antibacterial effects against both Gram-positive and negative bacteria. For instance, it was discovered that ZnO nanoparticles can hinder the growth of Staphylococcus aureus, whereas Ag nanoparticles demonstrate antibacterial action against E. coli and Pseudomonas aeruginosa, with the extent of this activity being dependent on the concentration of the nanoparticles [19]. Nevertheless, the precise antibacterial processes of NPs have not been fully elucidated, and similar types of NPs sometimes exhibit contradictory effects. The combination of CeO_2 and ZnO in nanoparticles can lead to synergistic effects, where the properties of the material may be superior to those of the individual components. For example, CeO_2 nanoparticles are known for their excellent catalytic properties, while ZnO nanoparticles exhibit semiconducting and photocatalytic properties. By combining these two materials, researchers aim to develop nanoparticles with enhanced functionalities for specific applications. In this work, the CeO_2-ZnO nanoparticles are prepared using a simple sol-gel process and their microstructural, optical, photocatalytic, and antibacterial activities are investigated.

2. MATERIALS AND METHODS

The chemicals utilized for this work were procured from M/s. Sigma Chemicals, USA. 3.669 grams of zinc acetate dihydrate ($Zn(CH_3CO_2)_2{\cdot}2H_2O$) was dissolved in de-ionized (DI) water, and then 8.684 grams of cerous nitrate hexahydrate ($Ce(NO_3)_3.6\ H_2O$) was dissolved in DI water separately. The two solutions were combined and 0.01 g of cetyltri methyl ammonium bromide (CTAB) was introduced as a surfactant. The mixture was then agitated for 30 min 2.10 grams of citric acid was dissolved in deionized water and the resultant solution was subsequently added gradually and continuously blended into the precursor solution. The specimen underwent desiccation by being placed in an oven at a temperature of 120 °C for a period of 24 h. Subsequently, it underwent an annealing at 600 °C for 2 h in a muffle furnace.

The sample's structure was analyzed using an X-ray diffractometer (XRD) equipped with CuKα radiation (Rigaku, Japan). The FTIR spectrometer (FTIR/ATR), was utilized for the analysis of bond vibrations in the sample. The surface morphology was examined using Field Emission Scanning Electron Microscopy (FESEM) (Carl Zeiss Microscopy Ltd, UK). The absorbance of the sample was analysed with the use of a double beam spectrophotometer (UV-1800, Shimadzu) in the 200 – 1000 nm wavelength region.

Antibiotics have a wide range of effectiveness against many types of bacteria. Penicillin was utilised as a control medication.

The antibacterial activity was evaluated using the standard approach of diffusion disc plates on agar, while the minimum inhibitory concentration (MIC) was obtained using the dilution method [20].

This was accomplished by the process of diluting the antibiotic substance in either agar or broth media. The technique of dilution susceptibility testing was utilised to determine the lowest quantity of antibiotic needed to impede or eliminate the microorganisms. The agar or broth media were used to dilute the antibiotic material in order to achieve this.

The Broth Dilution Method is a straightforward technique used to examine a limited number of isolates, including individual isolates.

The microorganisms employed in the study were strains of E. coli, Salmonella typhimurium, Bacillus cereus, and Shigella flexneri. The organisms E. coli (ATCC15224), Salmonella typhimurium (ATCC13048), Bacillus cereus (ATCC13061), and Shigella flexneri (ATCC12022) were sub-cultured in nutrient broth to get pure cultures. The specimens were individually introduced into a culture medium and incubated at 37 °C for a duration of 24 h. Subsequently, they were stored at a temperature of 4 °C until they were ready to be utilised.

Mueller-Hinton Agar is commonly considered the best option for conducting frequent susceptibility testing on non-fastidious bacteria since it consistently yields trustworthy results across several batches. It facilitates the optimal development of most low-maintenance infections. A significant volume of data and expertise has been accumulated about susceptibility investigations conducted utilising this medium.

The Mueller-Hinton Agar was prepared using the manufacturer's instructions. After autoclaving, the sample was then cooled in a water bath that was kept at a temperature of 45 – 50° range. The recently created and cooled medium was meticulously put into flat-bottomed Petri plates, made of either glass or plastic. This transfer was done on a surface that was both level and horizontal, ensuring that the depth of the medium in each dish was approximately 4 mm, consistently. The average capacity for plates measuring 150 mm in diameter is 60 – 70 ml,

whereas for plates measuring 100 mm in diameter, it is 25 – 30 ml. The agar medium was cooled to the surrounding temperature and, if not used immediately, stored in a refrigerator. Plates should be utilised within a week of being prepared, unless measures have been taken to prevent the drying of the agar, such as covering them with plastic. Each set of plates underwent sterility testing by incubating a representative sample at a temperature of 30 to 35 °C for at least 24 hours [21].

Discs of the two antibiotics such as Penicillin were used for this study. The nanoparticles were measured and used for the antibacterial studies.

Discs with a diameter of roughly 6 mm were created using Whattsman filter paper (No. 1). Subsequently, the discs were placed on a Petri plate and subjected to sterilization in a hot air oven. Following sterilisation, the discs were immersed in various concentrations of wide spectrum antibiotics and prepared nanoparticle solutions. They were then refrigerated for 24 hours [22].

In order to evaluate the adsorption of MB, CeO_2-ZnO catalyst (1g/1 L solution) was introduced to a solution containing 10 ppm of MB and stirred magnetically. Subsequently, the solution was kept in darkness for 30 min to establish an equilibrium. Next, a fluorescent lamp, was turned on to observe the degradation for a duration of 1 h. Following exposure to light, a 2 mL solution containing a mixture was collected at the specific time (15 min) intervals and centrifuged subsequently. Then, the spectrophotometer was used to analyse the absorption spectra of the solution. The photocatalytic performance is investigated utilising the photo reactor (HEBER, MODEL HVAR-MP400) under visible light conditions (550 nm wavelength and 125 watts) [23].

3. RESULTS AND DISCUSSION

3.1. Microstructural studies

XRD pattern of CeO_2/ZnO is shown in Fig. 1. The sharp diffraction peaks in the XRD pattern indicate that the prepared sample is polycrystalline. XRD pattern shows the peaks at angles 28.63° (111), 33.14° (200), 47.60° (220), 56.60° (311), 59.22° (222), 69.18° (400), 76.82° (331) and 79.10° (420) correspond to fcc structure of CeO_2.

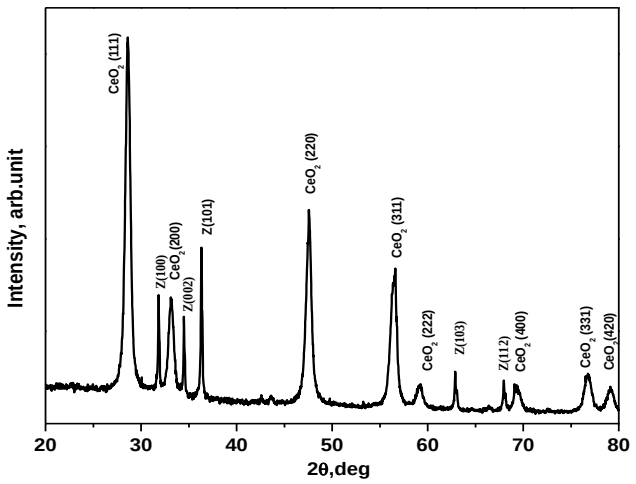

Fig. 1. XRD pattern of the CeO_2-ZnO nanoparticles

Also, there are peaks at angles 31.82° (100), 33.49° (002), 36.31° (101), 62.93° (103), 67.99° (112) belong to the ZnO with the hexagonal structure. It is observed that both CeO_2 and ZnO phases are present in the sample. XRD pattern shows the cubic structure ((JCPDS No. 34-394) of CeO_2 and hexagonal structure of ZnO (JCPDS No. 89-13971) respectively [1]. There were no more contaminant peaks detected in the sample. The crystallite sizes of ZnO and CeO_2 can be evaluated by the Scherer equation:

$$D = \frac{K\lambda}{\beta \cos\theta} . \quad (1)$$

where K=0.9, λ- incident wavelength, β-Full width at half maximum, θ-diffraction angle. The diameters of the crystallites were determined to be 18 nm and 29 nm for the nanoparticles of CeO_2 and ZnO, respectively. Chatchai Rodwihok et al [1] prepared the CeO_2 doped ZnO nanoparticle using a hydrothermal process and the XRD pattern indicated the ZnO of wurtzite and cubic CeO_2. Shen et al [15] Prepared the Ce doped ZnO composite by wet chemical method. The XRD patterns of the samples indicated the formation of CeO_2 of the fcc structure and ZnO of the wurtzite structure. Liang et al [24] prepared and examined Ce-doped ZnO, and XRD studies indicated that both the pure ZnO and Ce-doped ZnO samples possess a hexagonal structure. The results obtained in this study are consistent with previously reported findings.

FTIR spectrum of the CeO_2/ZnO nanoparticles (Fig. 2) demonstrates the existence of functional groups. The band observed at 2367 and 2179 cm^{-1} relates to the vibrational movements of O-H groups or the absorbed H_2O, specifically including stretching and bending. The bands detected at 1975 cm^{-1} and 1584 cm^{-1} can be attributed to remaining organic compounds [1, 25]. The frequencies at 650 cm^{-1} and 800 cm^{-1} demonstrate the characteristic elongation of Zn-O and O-Ce-O bonds, respectively.

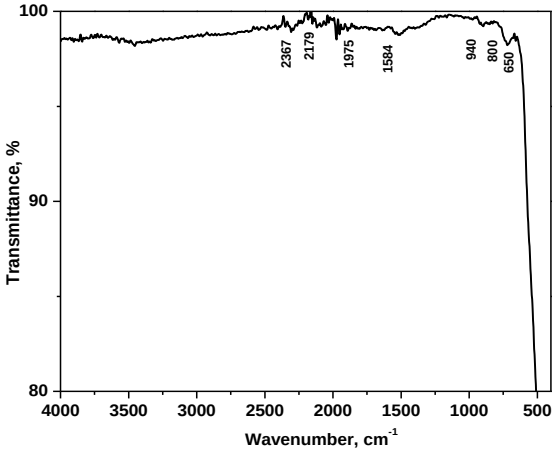

Fig. 2. FTIR spectrum of the CeO_2-ZnO nanoparticles

The sharp diffraction peaks in the XRD pattern indicate that the prepared sample is polycrystalline. XRD pattern shows the peaks at angles 28.63° (111), 33.14° (200), 47.60° (220), 56.60° (311), 59.22° (222), 69.18° (400), 76.82° (331) and 79.10° (420) correspond to fcc structure of CeO_2.

Fig. 3 shows the electron microscopy images of the CeO_2/ZnO NPs in different magnifications. These images demonstrated crystalline nature of the sample and dense structure with uniform size nanoparticles. It shows the photographs revealed the process of aggregation and agglomeration in the sample. The EDX examination verified the presence of cerium, zinc, and oxygen in the sample, and no additional contaminants have been detected [1, 25]. This demonstrates the effective incorporation of CeO_2 in ZnO matrix through doping.

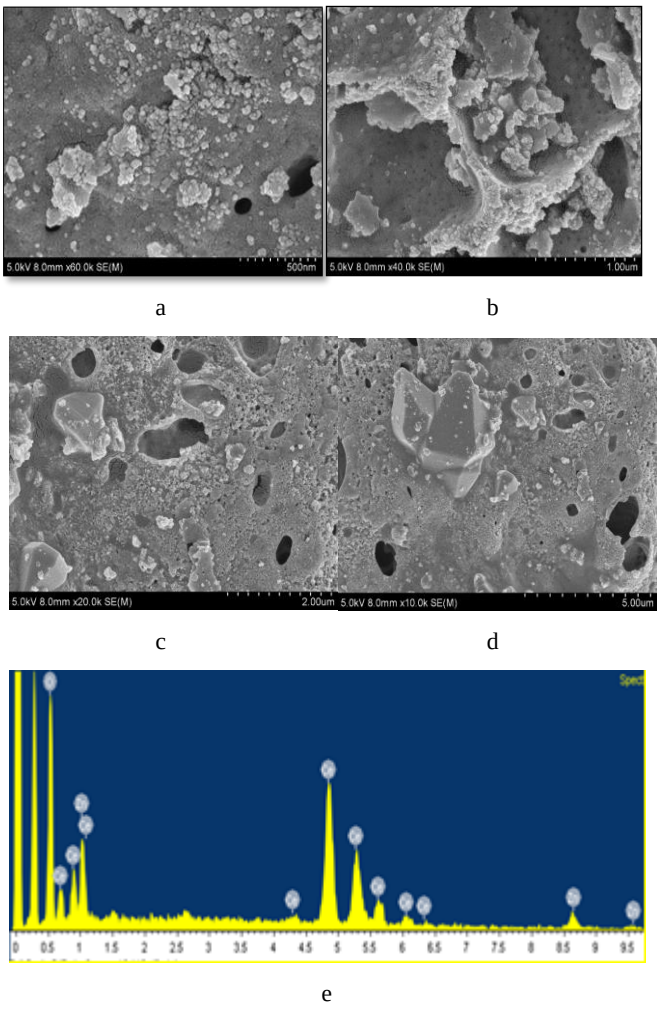

Fig. 3. a, b, c, d – FESEM images with different magnifications (60 K, 40 K, 20 K and 5 K); e – EDX spectrum of the CeO_2 doped ZnO NPs

3.2. Optical properties

The UV-Visible spectrophotometer was employed to evaluate the optical properties of the CeO_2/ZnO sample. Fig. 4 displays the absorption spectrum of the CeO_2/ZnO sample in its original state. A prominent absorption peak was seen at about 400 nm. The absorption coefficient (α) can be determined. The bandgap of the sample was calculated using the Tauc plot (Fig. 4 b). The determined bandgap of the CeO_2/ZnO sample is 3.15 eV. Chatchai Rodwihok et al studied the bandgap of a Ce/ZnO sample and found that the bandgap varies from 3.06 eV to 2.22 eV when Ce ions were introduced. These findings suggest that the addition of Ce reduces the bandgap of Ce/ZnO in comparison to pure ZnO, which has a positive effect on enhancing photocatalytic activity [1].

3.3. Photocatalytic studies

Dyes are crucial in the dyeing and textile sectors. The dyes utilized in several industries possess toxicity and carcinogenic properties, posing risks to both human health and marine ecology [26]. Hence, it is imperative to conduct an investigation into the repercussions of dyes being discharged into the environment [27]. The photocatalytic efficiency of the CeO_2-ZnO nanocatalyst is assessed based on its ability to degrade MB dye. Fig. 5 shows the photodegradation graph of the prepared sample on MB dye using visible light irradiation. The graph depicts the peak intensity level achieved by the MB dye at its distinctive wavelength.

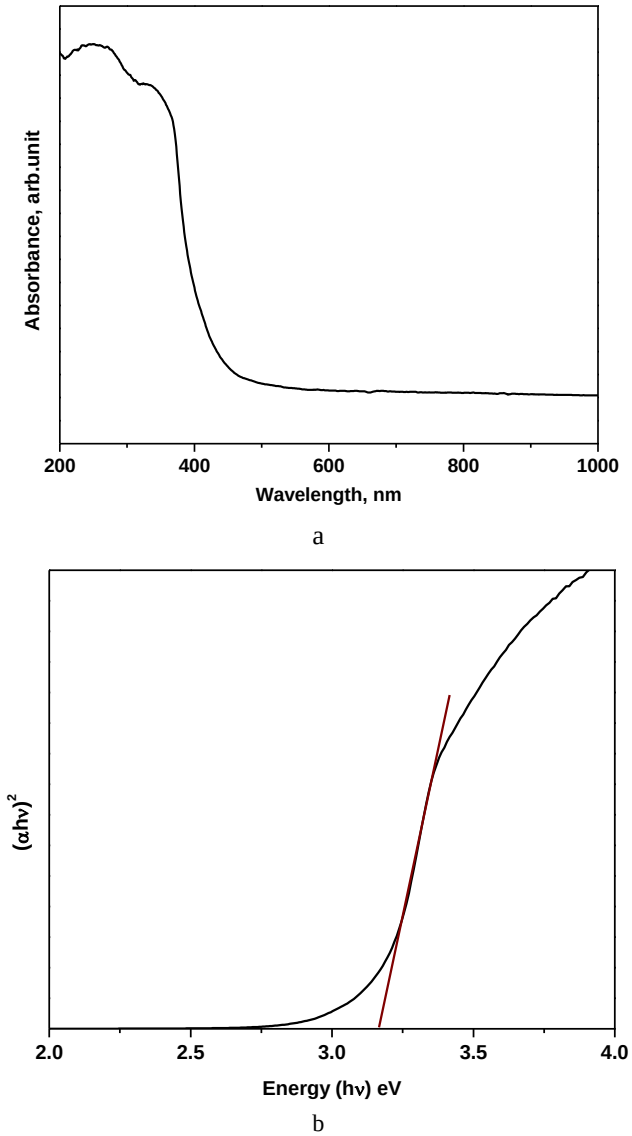

Fig. 4. UV-visible spectroscopy of the CeO_2-ZnO sample: a – absorption spectra; b – Tauc plot

The primary absorption peaks' intensity diminishes over time due to the degradation of dyes in the presence of nanoparticles, caused by their absorption in the visible spectrum. Due to its band gap of 3.15 e.V, this material effectively absorbs visible light [11]. The calculation of the

percentage of MB photodegradation is determined using the formula [17].

$$D = (A_0\text{-}A_t)/A_0 \times 100 \quad (2)$$

where A_0 and A_t are the initial and final absorbance values of MB, respectively and D is the degradation activity. The CeO_2/ZnO photocatalyst exhibited superior photocatalytic performance, achieving a degradation rate of 75.81 % for MB within a 60 min timeframe. The synthesized sample was found to be an excellent photocatalyst under visible light and showed promising results for MB dye degradation. Shen et al. prepared cerium-zinc oxide to degrade Rhodamine B (RhB) using photodegradation. The experiment showed 85.1 % degradation efficiency of RhB within 125 min.

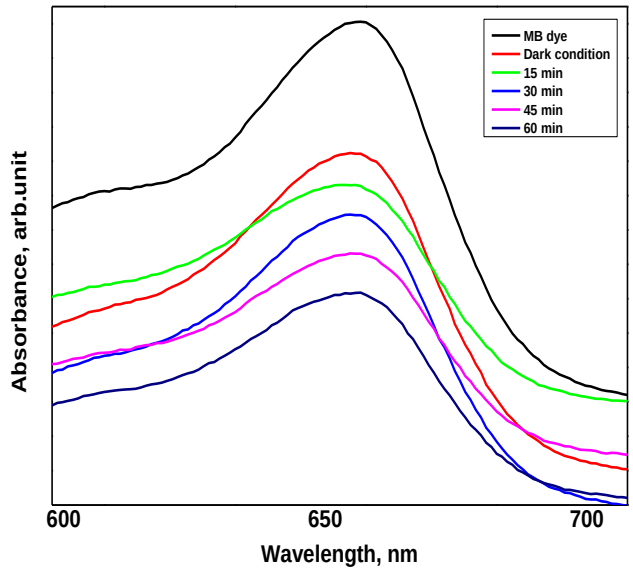

Fig. 5. Photocatalytic degradation of MB dye using CeO_2 doped ZnO catalyst

In addition, the formation of heterojunction, which serves as a charge separator to impede charge recombination and enhance the photodegradation [15]. The degradation efficiency for MB dye increased with Ce doping. The 0.03 wt.% Ce doped ZnO catalyst decolorized the MB dye in 120 min [28]. Chatchai Rodwihokv et al. [1] prepared the CeO_2 doped ZnO nanoparticles, and investigated the structural, optical, and catalytic activity of the samples. XRD pattern confirmed both the hexagonal structure of ZnO and cubic-phase CeO_2. The Ce/ZnO catalyst showed superior photodegradation of MO, with a degradation efficiency of 94 %.

3.4. Antibacterial activity

In recent studies, nanomaterials have shown significant promise as contrast agents for imaging the gastrointestinal tract and can disrupt infections caused by multidrug resistant bacteria [29]. When compared to small molecule antimicrobial agents, which have a limited duration of activity and often cause harm to the environment, nanoparticulate agents with antimicrobial activities have a longer duration of activity and cause low toxicity. Furthermore, research has demonstrated that the inhibition of Escherichia coli bacterial growth is negatively correlated with the size of the nanoparticles [30]. The CeO_2/ZnO nanoparticles are particularly intriguing among these agents due to their antibacterial characteristics [31]. The antibacterial mode of action is likely attributed to the induction of oxidative stress on the constituents of the cell membrane of microorganisms, particularly those of Gram-negative nature. The process of nanoparticles adsorption to the bacterium takes place when the location of infection has an acidic pH.

The present study investigated the antibacterial effects of CeO_2-ZnO NPs along with commercial antibiotic drug penicillin. Fig. 6 shows the minimum inhibitory concentration of 12 µg/ml in E. Coli. B. cereus shows moderate inhibition as compared to the S.typhi and S. flexneri. The NPs show significant antibacterial activity as compared to the control drug Penicillin at the concentration of 20 µg/ml. The results demonstrate that the nanoparticles exhibit substantial efficacy against specific microorganisms.

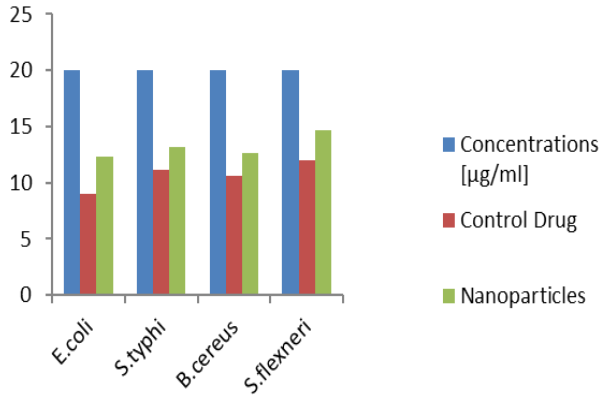

Fig. 6. The MIC of the control drug penicillin and CeO_2/ZnO nanoparticles at the concentration of 20 µg/ml

Maishara Syazrinni Rooshde et al. [17] prepared the CeO_2-ZnO and examined its antibacterial properties against E. coli and S. aureus using the agar well diffusion method. The findings indicated that the nanoparticles had both antibacterial properties and high photocatalytic efficiency. Syed et al prepared the nanocomposite and showed a degradation efficiency of 88 % when exposed to sunshine and 92 % for UV radiation for MO dye. CeO_2-ZnO NC demonstrated significant antibacterial action against a harmful bacterial strain [16]. Rabia Kırkgeçit et al prepared pure and CeO_2 doped ZnO particles using a sol-gel process and investigated the properties. XRD results showed the ZnO with a wurtzite structure. The optical properties revealed a bandgap of 2.94 – 3.07 eV. The results showed a photodegradation of 96.67 % for RhB dye [32]. In the two metal oxides, the formation of heterojunction reduces the recombination rate and improves the photocatalytic degradation performance [17].

4. CONCLUSIONS

CeO_2 doped ZnO nanoparticles were synthesised using a sol-gel process. XRD studies indicated the formation of both CeO_2 and ZnO phases belonging to the cubic and wurtzite structure respectively. The FTIR studies showed the presence of M-O-M bonds and confirmed the presence of metal oxides. FE-SEM analysis revealed the formation

of crystallites with agglomeration. EDX analysis confirmed the Ce, Zn, and O elements in the sample and there is no impurity. The bandgap of the CeO_2/ZnO sample was found to be 3.15 eV as shown in the Tauc plot. The CeO_2-ZnO nanoparticles exhibited a higher 75.81 % degradation efficiency for MB dye under visible light irradiation. The CeO_2-ZnO nanoparticles showed significant antibacterial activity as compared to the control drug penicillin.

REFERENCES

1. **Rodwihok, C., Wongratanaphisan, D., Tam, T.V., Choi, W.M., Hur, S.H., Chung, J.S.** Cerium Oxide Nanoparticle Decorated Zinc Oxide with Enhanced Photocatalytic Degradation of Methyl Oange *Applied Sciences* 10 (5) 2020: pp. 1697 – 2010. https://doi.org/10.3390/app10051697
2. **Liu, J., Hong, Ye., Tian, X., Meng, X., Gao, G., He, T., Nie, Y., Jin, G., Zhai, Z., Fu, C.** Semiconductor Photocatalyst of Tin Oxide Quantum Dots Prepared in Aqueous Solution for Degradation of Organic Pollutants in Contaminated Water *Materials Science (Medžiagotyra)* 28 (1) 2022: pp. 30 – 34. https://doi.org/10.5755/j02.ms.25558
3. **Gnanam, S., Shynu, R.K., Gajendiran, J., Ramana Ramya, J., Thennarasu, G., Thanigai Arul, K., Gokul Raj, S., Ramesh Kumar, G.** Synthesis and Characterization of ZnO-NiO Nanocomposites for Photocatalytic and Electrochemical Storage Applications *Ionics* 2024: pp. 1 – 13. https://doi.org/10.1007/s11581-024-05728-6
4. **Kumaravelu, T.A., Ta, T.T.N., Chung-Li, D., Wu-Ching, C.** Water Photo- and Electro-Catalysis: Mechanisms, Materials, Devices, and Systems, 2024: Chapter 10 *Advanced X-ray Absorption Spectroscopy on Electrocatalysts and Photocatalysts.* https://doi.org/10.1002/9783527831005.ch10
5. **Ramana Ramya, J., Thanigai Arul, K., Karthikeyan, K.R., Nabhiraj, P.Y., Krishna, J.B.M., Kaarthikeyan, G., Sathiamurthi, P., Gajendiran, J., Chung-Li, D., Narayana Kalkura, S.** Surface Modification of Iron-Zinc Ions Incorporated Calcium Phosphate Biocomposite Flexible Films for Biomedical Applications *Materials Today Communications* 38 2024: pp. 107988. https://doi.org/10.1016/j.mtcomm.2023.107988
6. **Khalid, N., Hammad, A., Tahir, M., Rafique, M., Iqbal, T., Nabi, G., Hussain, M.** Enhanced Photocatalytic Activity of Al and Fe co-doped ZnO Nanorods for Methylene blue Degradation *Ceramics International* 45 (17) 2019: pp. 21430 – 21435. https://doi.org/10.1016/j.ceramint.2019.07.132
7. **Motla, A., Kumaravelu, T., Dong, C.L., Kandasami, A., Avasthi, D.K., Annapoorni, S.** Structural and Optical Tunability of Ag-ZnO Nanocomposite Thin Films for Surface-enhanced Raman Studies *Plasmonics* 19 2024: pp. 335 – 345. https://doi.org/10.1007/s11468-023-01965-z
8. **Motla, A., Kumaravelu, T.A., Dong, C.L., Chen, C.L., Asokan, K., Annapoorni, S.** Role of Annealing Environments on the Local Electronic and Optical Properties of Zinc Oxide Films *Journal of Materials Science: Materials in Electronics* 35 2024: pp. 267. https://doi.org/10.1007/s10854-024-12018-4
9. **Poornaprakash, B., Chalapathi, U., Sekhar, M.C., Rajendar, V., Vattikuti, S.P., Reddy, M.S.P., Suh, Y., Park, S.H.** Effect of Eu3+ on the Morphology, Structural, Optical, Magnetic, and Photocatalytic Properties of ZnO Nanoparticles *Superlattices Microstructures* 123 2018: pp. 154 – 163. https://doi.org/10.1016/j.spmi.2018.07.010
10. **Hemalatha, P., Karthick, S., Hemalatha, K., Yi, M., Kim, H.J., Alagar, M.** La-doped ZnO Nanoflower as Photocatalyst for Methylene Blue Dye Degradation Under UV irradiation *Journal of Materials Science: Materials in Electronics* 27 2016: pp. 2367 – 2378. https://doi.org/10.1007/s10854-015-4034-8
11. **Tang, W.X., Gao, P.X.** Nanostructured Cerium Oxide: Preparation, Characterization, and Application in Energy and Environmental Catalysis *MRS Communications* 6 2016: pp. 311 – 329. https://doi.org/10.1557/mrc.2016.52.ELIAS
12. **Elias, J.S., Risch, M., Giordano, L., Mansour, A.N., Shao-Horn, Y.** Structure, Bonding, and Catalytic Activity of Monodisperse,Transition-Metal-Substituted CeO_2 Nanoparticles *Journal of American Chemical Society* 136 (49) 2014: pp. 17193 – 17200. https://doi.org/10.1021/ja509214d
13. **Kallappa, D., Venkatesha, T.V.** Synthesis of CeO_2 Doped ZnO Nanoparticles and Their Application in Zn-Composite Coating on Mild Steel *Arabian Journal of Chemistry* 13 (1) 2020: pp. 2309 – 2317. https://doi.org/10.1016/j.arabjc.2018.04.014
14. **Xie, Q., Zhao, Y., Guo, H., Lu, A., Zhang, X., Wang, L., Chen, M.S., Peng, D.L.** Facile Preparation of Well-Dispersed CeO_2–ZnO Composite Hollow Microspheres with Enhanced Catalytic Activity for CO Oxidation *ACS Applied Materials and Interfaces* 6 (1) 2014: pp. 421 – 428. https://doi.org/10.1021/am404487b
15. **Shen, Z., Zhang, Q., Yin, C., Kang, S., Jia, H., Li, X., Li, X., Wang, Y., Cui, L.** Facile Synthesis of 3D flower-like Mesoporous Ce-ZnO at Room temperature for the Sunlight-driven Photocatalytic Degradations of RhB and Phenol *Journal of Colloidal and Interface Science* 556 2019: pp. 726 – 733. https://doi.org/10.1016/j.jcis.2019.08.111
16. **Syed, A., Yadav, L.S.R., Bahkali, A.H., Elgorban, A.M., Abdul Hakeem, D., Ganganagappa, N.** Effect of CeO_2-ZnO Nanocomposite for Photocatalytic and Antibacterial Activities *Crystals* 10 (9) 2020: pp. 817. https://doi.org/10.3390/cryst10090817
17. **Rooshde, M.S., Abdullah, W.R.W., Amran, AZ., Ibrahim, N.F., Ariffin, F., Ghazali, M.S.M**. Antimicrobial Activity of Photoactive Cerium Doped Zinc Oxide *Solid State Phenomena* 307 (10) 2020: pp. 217 – 222. https://doi.org/10.4028/www.scientific.net/SSP.307.217
18. **Ramalingam, B., Parandhaman, T., Das, S.K**. Antibacterial Effects of Biosynthesized Silver Nanoparticles on Surface Ultrastructure and Nanomechanical Properties of Gram-negative Bacteria viz. Escherichia coli and Pseudomonas aeruginosa *ACS Applied Material Interfaces* 8 (7) 2016: pp. 4963 – 4976. https://doi.org/10.1021/acsami.6b00161
19. **Jung, WK., Koo, H.C., Kim, KW., Shin, S., Kim, S.H., Park, Y.H.** Antibacterial Activity and Mechanism of Action of the Silver Ion in Staphylococcus aureus and Escherichia coli *Applied* and *Environmental Microbiology* 74 (7) 2008: pp. 2171 – 2178. https://doi.org/10.1128/AEM.02001-07

20. **Bauer, A., Kirby, W.M.M., Sherris J.C., Turck M.** Antibiotic Susceptibility Testing by a Standardized Single Disk Method *American Journal of Clinical Pathology* 45 (4) 1966: pp. 493 – 496. https://doi.org/10.1093/ajcp/45.4_ts.493

21. **Liao, S., Zhang, Y., Pan, X., Zhu, F., Jiang, C., Liu, Q., Cheng, Z., Dai, G., Wu, G., Wang, L., Chen, L.** Antibacterial Activity and Mechanism of Silver Nanoparticles Against Multidrug-resistant *Pseudomonas aeruginosa* *International Journal of Nanomedicine* 25 (14) 2019: pp. 1469 – 1487. https://doi.org/10.2147/IJN. S191340

22. **Ahmed, S., Ahmad, M., Swami, B.L., Ikram, S.** A review on Plants Extract Mediated Synthesis of Silver Nanoparticles for Antimicrobial Applications: A Green Expertise *Journal of Advanced Research* 7 (1) 2016: pp. 17 – 28. https://doi.org/10.1016/j.jare.2015.02.007

23. **Wang, Y., Balakrishnan, G.** Microstructural, Antifungal and Photocatalytic Activity of NiO–ZnO Nanocomposite *Materials Science-Poland* 42 (1) 2024: pp. 107 – 115. https://doi.org/10.2478/msp-2024-0006

24. **Liang, Y., Guo, N., Li, L., Li, R., Ji, G., Gan, S.** Preparation of Porous 3D Ce-doped ZnO Microflowers with Enhanced Photocatalytic Performance *RSC Advances* 5 2015: pp. 59887 – 59894. https://doi.org/10.1039/C5RA08519E

25. **Alabyadh, T., Albadri, R., Es-Haghi, A., Yazdi, M.E.T., Ajalli, N., Rahdar, A., Thakur, V.K.** ZnO/CeO_2 Nanocomposites: Metal-Organic Framework-Mediated Synthesis, Characterization and Estimation of Cellular Toxicity toward Liver Cancer Cells *Journal of Functional Biomater*ials 13 (3) 2022: pp. 139. https://doi.org/10.3390/jfb13030139

26. **Zollinger, H.** Color Chemistry: Syntheses, Properties, and Applications of Organic Dyes and Pigments Third revised Edition, Wiley-VCH, 2003.

27. **Robinson, T., Mcmullan G., Marchant R., Nigam, P.** Remediation of Dyes in Textile Effluent: A Critical Review on Current Treatment Technologies with a Proposed Alternative *Bioresource Technology* 77 (3) 2001: pp. 247 – 255. https://doi.org/10.1016/S0960-8524(00)00080-8

28. **Shanthi, K., Kalyani Veena, B., Navneetha, P., Potharaju, K., Vardhani, C.** Photocatalytic Degra,dation of Methylene Blue Dye Using Cerium Doped Zinc Oxide Nanoparticles *Sådhanå* 45 2020: pp. 128 – 136. https://doi.org/10.1007/s12046-020-01329-x

29. **Yang, X., Junchuan, Y., Le, W., Bei, R., Yuexiao, J., Lingmin, Z., Guang, Y., Huawu, S., Xingyu, J.** Pharmaceutical Intermediate-Modified Gold Nanoparticles: Against Multidrug-Resistant Bacteria and Wound-Healing Application via an Electrospun Scaffold *ACS Nano* 11 (6) 2017: pp. 5737 – 5745. https://doi.org/10.1021/acsnano.7b01240

30. **Pelletier, D.A., Suresh, A.K., Holton, G.A., McKeown, C.K., Wang, W., Gu, B., Mortensen, N.P., Allison, D.P., Joy, D.C., Allison, M.R., Brown, S.D., Phelps, T.J., Doktycz, M.J.** Effects of Engineered Cerium Oxide Nanoparticles on Bacterial Growth and Viability *Applied and Environmental Microbiology* 76 (24) 2010: pp. 7981 – 7989. https://doi.org/10.1128/AEM.00650-10

31. **Zhang, M., Chao, Z., Xinyun, Z., Feng, L., Yaping, Du., Chunhua, Y.** Antibacterial Mechanism and Activity of Cerium Oxide Nanoparticles *Science China Materials* 62 2019 pp. 17271 – 1739. https://doi.org/10.1007/s40843-019-9471-7

32. **Kirkgeçit, R., Kavgacı, M., Soğuksu, A., Kerli, S., Torun, H**. Photocatalytic Degradation Effect of Rhodamine B dyes on Cerium Oxide Doped Zinc Oxide Particles Under Visible Light Irradiation *Environmental Engineering and Management Journal* 21 (8) 2022: pp. 1363 – 1372. https://doi.org/10.30638/eemj.2022.121